

Twist-Controlled Force Amplification and Spinning Tension Transition in Yarn

Antoine Seguin 

Université Paris-Saclay, CNRS, FAST, 91405, Orsay, France

Jérôme Crassous *

Université Rennes, CNRS, IPR (Institut de Physique de Rennes)—UMR 6251, F-35000 Rennes, France



(Received 24 August 2021; accepted 19 January 2022; published 18 February 2022)

Combining experiments and numerical simulations with a mechanical-statistical model of twisted yarns, we discuss the spinning transition between a cohesionless assembly of fibers into a yarn. We show that this transition is continuous but very sharp due to a giant amplification of frictional forces which scales as $\exp\theta^2$, where θ is the twist angle. We demonstrate that this transition is controlled solely by a nondimensional number \mathcal{H} involving twist, friction coefficient, and geometric lengths. A critical value of this number $\mathcal{H}_c \simeq 30$ can be linked to a locking of the fibers together as the tensile strength is reached. This critical value imposes that yarns must be very slender structures with a given pitch. It also induces the existence of an optimal yarn radius. Predictions of our theory are successfully compared to yarns made from natural cotton fibers.

DOI: [10.1103/PhysRevLett.128.078002](https://doi.org/10.1103/PhysRevLett.128.078002)

Yarns made from natural fibers are one of the first materials ever processed by humans, including Neanderthals [1]. They are done by making bundles of initially aligned fibers which are then stuck together by twisting. The fact that many individual fibers of a few centimeters may form yarns of tens of meters drew early attention from scientists. Galileo [2] argued that the twist “binds” the filaments together, but did not discuss the origin of this cohesion. We now know that the binding forces are created by the tension throughout the filaments which creates normal forces due to the curvatures of the fibers, and that tangential frictional forces prevent sliding of fibers [3–5]. If the twist is large enough, the relative sliding of fibers is totally blocked, and the rupture of the yarn is then a problem of statistic of rupture of individual fibers [6,7]. The description of the transition between fibers which are “free to slide” without spinning, to “blocked by spinning” is still an open problem. Experimentally, only very few studies addressed the dependence of yarn strength with twist level [8]. Theoretically, despite numerous attempts, the mechanism linking twist and strengthening has not been clearly understood [9–13]. Recently, an analogy with the percolation transition had been suggested [14]. Assembly of fibers is an example of assembly of objects that interact through numerous frictional contacts. For such systems, the geometrical arrangement of the contact points may generate huge stress throughout the system. Some examples of such systems are granular materials in proximity to a solid wall (Jansen effect [15,16]), assembly of parallel sheets in contact (interleaved phone book experiment [17,18]), or contact points distributed around a cylinder (capstan). In all of those examples,

the proportionality between the tangential and the normal stress at contact means that the mechanical stress in the system decreases exponentially with the distance to the applied load, and then has drastic effects of the mechanical equilibrium of such a system.

We show in this Letter that an assembly of fibers belongs to the same class of system. For this, we consider model yarns made of entangled twisted fibers. The tension necessary to unravel the fibers is shown to vary continuously, but very rapidly with the twist. This sharp evolution of the disentanglement force creates a phase transition like the transition between the free fiber and stuck fiber phases. A simple mechanical model of frictional helicoidal fibers allows us to define a nondimensional number whose value characterizes this transition. These results can be successfully applied to real yarns.

Experimental model yarn system.—Our starting point is the demonstrating experiment of friction force in yarns as proposed by Bouasse [4]. We consider two brushes of $N/2$ identical fibers [see Fig. 1(a)]. The fibers are passed through rings which are connected to puller jaws ($N/2$ fibers in each jaw). The model fibers are of flexible strings of cotton (diameter $d = 1$ mm, linear density $\lambda = 0.48$ g m⁻¹, friction coefficient $\mu_m = 0.35$, bending modulus $B \sim 10^{-6}$ N m²), or flax ($d = 1$ mm, $\lambda = 1.03$ g m⁻¹, $\mu_m = 0.53$, $B \sim 4.10^{-6}$ N m²). The twist of the elementary yarns composing each string is always very large compared to the twist that we apply. We first prepare the entanglement by alternately aligning the brushes roughly parallel. The brushes are then zipped together with two plastic cable clamps, and twisted by a angle θ [Figs. 1(b) and 1(c)]. The puller jaws are attached to a traction measurement apparatus (Instron 5965,

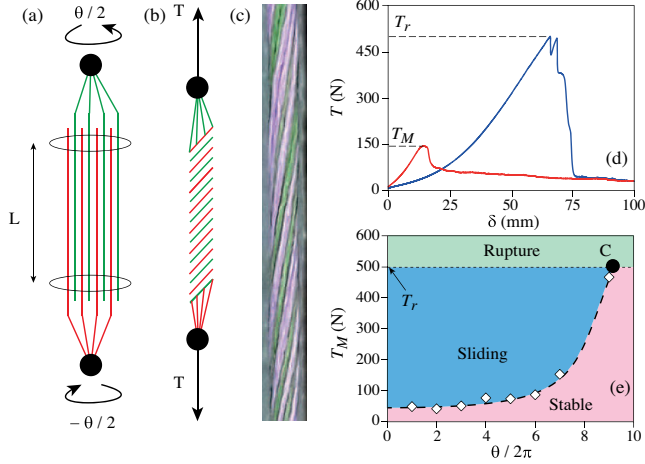


FIG. 1. (a),(b) Preparation of the model yarn before (a) and after (b) twisting. (c) Photo of a yarn made from cotton strings after twisting. (d) Traction forces as a function of displacement for cotton yarn $L = 800$ mm: (blue) $\theta/2\pi = 11$, (red) $\theta/2\pi = 3$. (e) Symbol: maximum traction force as full twist angles (cotton yarn, $L = 800$ mm), dotted line is a guide for the eye, and dashed line is the rupture force.

5 kN force sensor) and elongated at fixed velocity 50 mm min^{-1} . Figure 1(d) shows the force variations for two different twist angles. If the twist angle is low enough, the force first increases, reaches a peak value (noted T_M), and then decreases slowly. Such variations are associated with a smooth relative sliding of the two brushes. For large enough twist, a force drop is measured after the maximum force (noted T_r). This is associated with the rupture of one or many strings that we may observe by postmortem inspection. Figure 1(e) shows the evolution of T_M as a function of the twist angle. This value is likely constant up to $\theta/2\pi \simeq 5$ revolutions for this yarn, and increases rapidly up to nine revolutions where T_M reaches T_r at point C.

Scaling laws for maximum traction.—We first limit our analysis to the maximum force T_M and we do not discuss rupture. Since we expect that the maximum force is dependent on friction, T_M should depend on μ_m and of geometric characteristics of the yarn: θ , L , R , and N . We define the twist rate $\gamma = R\theta/L \ll 1$.

We first discuss the γ dependence of T_M . Noting T_0 the traction force at vanishing twist, we must have $T_M(\gamma) = T_0 F(\gamma)$, or $\ln(T_M) = \ln(T_0) + f(\gamma)$ with $f = \ln(F)$ an even function vanishing at $\gamma = 0$. The leading term of expansion at small twist is $f \sim \gamma^2$. This dependence is experimentally verified as shown on Fig. 2(a). It follows that

$$\ln(T_M/T_0) = \gamma^2 g(L/R, N, \mu_m), \quad (1)$$

where g is a nondimensional function of nondimensional parameters. The L/R dependence of g is obtained by considering the evolution of traction force at fixed θ , R , and N and of various lengths L . We found [see Fig. 2(b)]

that $g(L/R, N, \mu_m) \sim L/R$, so that $\ln(T_M/T_0) = (\gamma^2 L/R) h(N, \mu_m)$.

Numerical yarn.—We use discrete element method simulations [19] to obtain the function h . Fibers are modeled as a set of point masses connected with elongational spring and dashpot without torsional or bending restoring forces. Successive masses are connected with cylinders of diameter d . The contact points between cylinders (belonging to same or different fibers) are calculated, and the contact forces are calculated considering normal stiffness and damping, and tangential stiffness with Coulomb friction coefficient μ_m . Equations of motion are integrated using a Verlet algorithm. The steps for making numerical yarns are depicted in Fig. 2. We first stretch the N fibers under a force t_0 [Fig. 2(d)] such that the strain of each fiber is 10^{-4} . A torque is then applied to the yarn by submitting both ends of fibers to orthoradial forces s [Fig. 2(e)]. During this preloading phase, μ_m is kept to a low value 0.05 which ensures a uniform twist along the yarn [Fig. 2(g)]. Finally, while keeping forces t_0 and s applied, the tension t of half the fibers on the bottom and to the other half at the top [Fig. 2(f)] is slowly increased until a value $t = t_M$ where the brush separates.

Full symbols of Fig. 2(c) show the evolution of t_M/t_0 with the twist angle for different values of μ_m and N . First, we obtain that $\ln(t_M/t_0) \sim \theta^2$ as for experimental data. We have also checked (data not shown here) that $g \sim L/R$. The friction coefficient μ_m is varied, and the N dependency is obtained from simulations of N fibers of radius a_N such that $R = a_N \sqrt{N/\phi}$ (with $\phi = 0.80$ the packing fraction) ensuring fixed string radius R . We did not identify significant variations with N between $N = 20$ and $N = 100$ [Fig. 2(c)].

Finally, Fig. 2(c) shows that all the experimental and numerical data may be collapsed using the single law:

$$T_M/T_0 = \exp\left(0.75\mu\theta^2 \frac{R}{L}\right), \quad (2)$$

with $\mu = 0.63 \mu_m$ for laboratory and $\mu = 1.13 \mu_m$ for numerical experiments. The experimental dependence on μ_m may be viewed on Fig. 2(c) where data for flax and cotton collapse when plotted as a function of $\mu\theta^2 R/L$. Finally, the amplification of the tension in the yarn is thus exponential, and only related to a dimensionless number $\mathcal{H} = \mu\theta^2 R/L$ that we name the ‘‘Hercules twist number.’’

Mechanical model.—We develop a mechanical model for deriving (2). We consider a yarn made of N helicoidal fibers [Fig. 3(a)] with some rising and descending fibers. We consider first a twisted fiber at a distance r from the axis: $\mathbf{r} = r\mathbf{e}_\rho + z\mathbf{e}_z$ in cylindrical coordinates (ρ, φ, z) [Fig. 3(b)]. The geometry of the helix of constant pitch P gives $\varphi/2\pi = z/P$ and we define the reduced pitch as $p = P/2\pi$. For pitch large compared to r , the tangent vector of the fiber is $\mathbf{e}_t(z) \simeq r/p\mathbf{e}_\varphi + \mathbf{e}_z$. The tension is $\mathbf{t}(z) = t(z)\mathbf{e}_t(z)$, and

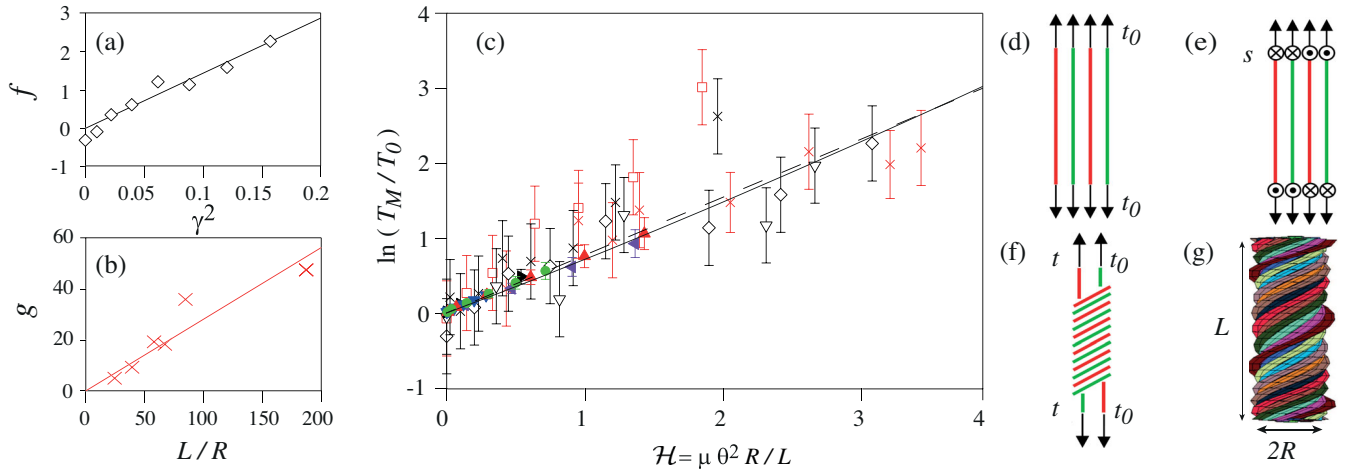


FIG. 2. (a) Scaling law $f(\gamma^2)$ for cotton yarn at fixed R and L . Line is linear fit. (b) Scaling law $g(L/R)$ for flax yarn at fixed twist $\theta = 2.5$ turns. Line is linear fit. (c) $\ln(T_M/T_0)$ as function \mathcal{H} . Dashed line is Eq. (2), plain curve is Eq. (6b). For (a)–(c) Crosses and open symbols are experimental data. Cotton, $N = 20$, $R = 3.15$ mm: $L = 200$ mm (down pointing white triangle), $L = 400$ mm (diamond), $L = 200$ mm (down pointing white triangle). Flax, $N = 20$, $R = 4.15$ mm: $L = 400$ mm, various θ (solid red square), $\theta = 2.5$ turns, various L (red cross mark). Plain symbols are numerical data with $L/R = 60$: $\mu_m = 1$, $N = 40$ (up pointing orange triangle), $\mu_m = 0.5$, $N = 40$ (green filled circle), $\mu_m = 0.5$, $N = 20$ (left pointing violet triangle), $\mu_m = 0.5$, $N = 100$ (right pointing black triangle), $\mu_m = 0.2$, $N = 40$ (down pointing blue triangle). (d)–(f) Schematic drawing of the preparation of the numerical yarn: (d) uniform tension t_0 is applied; (e) Shear force s is applied to twist the yarn; (f) Tension is increased to t on the top of half fibers, and on the bottom of the other fibers. (g) Snapshot of a brush of fibers after twisting, and during the increase of t ($N = 20$, $L/R = 60$). Note the difference of vertical and horizontal scales.

$$\frac{d\mathbf{t}}{dz} = \frac{dt}{dz} \mathbf{e}_t - \frac{r}{p^2} t(z) \mathbf{e}_\rho \simeq \frac{dt}{dz} \mathbf{e}_z - \frac{r}{p^2} t(z) \mathbf{e}_\rho. \quad (3)$$

We first consider the force equilibrium, in a section of the yarn, for a portion of fiber between z and $z + dz$. The force $-(rdz/p^2)t(z)\mathbf{e}_\rho$ is a linear restoring force toward the axis of the yarn: the torsion of the yarn is then equivalent putting the fiber into a twist-controlled harmonic potential $V(r) = t(z)dz(r^2/2p^2)$. At mechanical equilibrium, contact forces must balance this confining force. The equilibrium of forces in the plane perpendicular to the fiber writes

$$\frac{r}{p^2} t(z) \mathbf{e}_\rho = \sum_{j=1}^{\mathcal{N}} f_n^{(j)} \mathbf{e}_n^{(j)}, \quad (4)$$

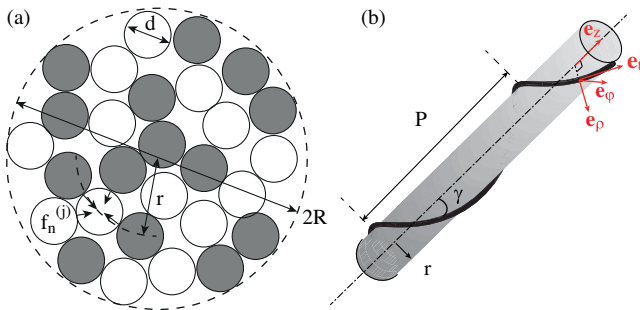


FIG. 3. (a) Section of a yarn of radius R composed of fibers of diameter d . Gray fibers go downward and white fibers go upward. (b) A fiber twisted on a cylinder of radius r .

with \mathcal{N} the number of contacts, $f_n^{(j)} dz \mathbf{e}_n^{(j)}$ the contact force between z and $z + dz$ exerted by fiber j , and $\mathbf{e}_n^{(j)}$ the normal vectors at contact points. Let f_n be the order of magnitude of normal forces $f_n^{(j)}$. Since vectors $\mathbf{e}_n^{(j)}$ have random orientations, the right-hand side of (4) may be viewed as a $2d$ random walk in force space, and we should have $t(z)r/p^2 \sim \sqrt{\mathcal{N}}f_n$. We now consider the force along z of the rising fiber due to the $\mathcal{N}/2$ fibers that do not rise. Each contact exerts a sliding force $\simeq \mu_m f_n$, and then $(dt/dz) \simeq (\mathcal{N}/2)\mu_m f_n \simeq (\sqrt{\mathcal{N}}/2)\mu_m t(z)r/p^2$. We finally obtain

$$\frac{dt}{dz} = \mu \frac{r}{p^2} t(z), \quad (5)$$

with $\mu = (\sqrt{\mathcal{N}}/2)\mu_m$. The coordination number for a random close packing of disks being 4 [20], we should have $\mu \simeq \mu_m$, in agreement with laboratory and numerical experiments. Integrating (5) along z gives $t(L) = t_0 \exp(\mu r L/p^2)$. Using $\theta = L/p$, and $dN(r)/dr = Nr/R^2$ the density of rising fibers, the force on the yarn section is

$$T_M = \int_{r=0}^{r=R} t_0 \exp\left(\mu \theta^2 \frac{r}{L}\right) dN(r) \quad (6a)$$

$$= T_0 \frac{2[(\mathcal{H} - 1) \exp \mathcal{H} + 1]}{\mathcal{H}^2}, \quad (6b)$$

where $T_0 = Nt_0/2$, and with \mathcal{H} the Hercules twist number \mathcal{H} previously defined. Since t_0 is only in prefactor of the

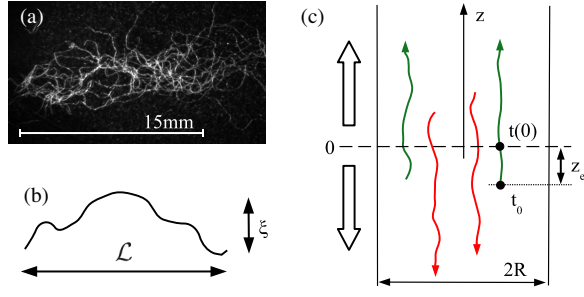


FIG. 4. (a) Fibers of cotton. (b) Length \mathcal{L} and tortuosity ξ of fiber. (c) Separation of a yarn at a plane $z = 0$. Arrows show the directions relative to the plane $z = 0$.

exponential amplification, the scaling $\ln(T_M/T_0) \sim \mathcal{H}$ is expected to hold if (6a) is extended to a radius dependant tension $t_0(r)$, as it is the case for dense packing of twisted fibers [21], or if there is disorder on the values of t_0 .

Staples yarn.—We now apply our results to a yarn made of an assembly of fibers of length \mathcal{L} as shown in Fig. 4. Figure 4(c) shows a yarn which separates in two parts from an arbitrary plane $z = 0$. A fiber with center located above this plane rises. Let z_e be the distance between the end of the fiber and the plane, and t_0 the tension at the end of the fiber. Integrating (5) from $-z_e$ to 0 gives $t(z = 0) = t_0 \exp(\mu r z_e / p^2)$. By symmetry, the relation is the same for a descending fiber. Noting $\mathcal{P}(z_e) dz_e$ the probability that fiber ends at a distance between z_e and $z_e + dz_e$, the total separating force is then

$$T_M = \int_{r=0}^{r=R} dN(r) \int_{z_e} t_0 \exp(\mu r z_e / p^2) \mathcal{P}(z_e) dz_e \quad (7a)$$

$$= N t_0 \frac{2\{\exp(\mathcal{H}/2) - [1 + (\mathcal{H}/2)]\}}{(\mathcal{H}/2)^2}, \quad (7b)$$

where $\mathcal{H} = \mu R \mathcal{L} / p^2$. We used $dN(r) = 2N r dr / R^2$ with N the number of fiber in one section, and assumed a uniform distribution of ends of fibers $\mathcal{P}(z_e) = 2/\mathcal{L}$ for $0 \leq z_e \leq \mathcal{L}/2$. The tension $N t_0$ that the yarn may support without twist is then amplified by a factor $A(\mathcal{H}) = 2\{\exp(\mathcal{H}/2) - [1 + (\mathcal{H}/2)]\} / (\mathcal{H}/2)^2$. We expect that the exponential amplification still occurs for various distribution $\mathcal{P}(z_e)$: i.e., taking $\mathcal{P}(z_e)$ as a Dirac distribution $\delta(z_e - L)$ in (7a), we recover (6b). Exponential amplification should also occur in case of disordered values of t_0 , or if fibers trajectories are not perfectly helicoidal.

Critical Hercules twist number and spinning transition.—This amplification factor $A(\mathcal{H})$ increases nearly exponentially with \mathcal{H} . However, the maximum traction T_M cannot be larger that the force T_r for which the rupture of the fibers occurs. We note \mathcal{H}_c the critical value of the Hercules twist number which verifies $T_r = N t_0 A(\mathcal{H}_c)$. It occurs at a point C on Fig. 1(e). \mathcal{H}_c separates weakly twisted yarns ($\mathcal{H} < \mathcal{H}_c$) that fail by sliding of fibers,

from highly twisted yarns ($\mathcal{H} > \mathcal{H}_c$) that fail by breaking of fibers.

A typical value of \mathcal{H}_c for a yarn made of identical fibers of diameter d and of length \mathcal{L} may be evaluated. Noting E the Young's modulus, and ε_r the deformation of fibers at rupture, and dropping constant numerical factor, the rupture tension is $t_r \sim \varepsilon_r E d^2$ for a fiber, and $T_r = N t_r$ for a yarn. Since fibers are slender objects, we take t_0 as the force necessary to straighten into a yarn the fibers that are initially bent. Noting ξ the initial flexion of the fibers [Fig. 4(b)] we have $t_0 \sim E d^4 \xi / \mathcal{L}^3$. It follows that $A(\mathcal{H}_c) = t_r / t_0 \sim \varepsilon_r \mathcal{L}^3 / \xi d^2$. For cotton fibers with $\mathcal{L} = 30$ mm, $d = 16$ μm , $\mu_m = 0.48$ [22,23], $\varepsilon_r \simeq 0.08$, and $\xi \sim \mathcal{L}/3$: $A(\mathcal{H}_c) \sim 10^5$, and $\mathcal{H}_c \simeq 33$. The associated pitch for a yarn of radius $R = 80$ μm is $P = 2\pi \sqrt{\mu R \mathcal{L} / \mathcal{H}_c} \simeq 1.2$ mm. From a microscopic inspection of the yarn, we measured a similar value of the pitch $P \simeq 1.5$ mm. For fibers made of an identical material with $\xi \sim \mathcal{L}$, and dropping nonexponential term in $A(\mathcal{H}) \sim \exp(\mathcal{H}/2)$, we obtain the simple scaling $\mathcal{H}_c \sim 4 \ln(\mathcal{L}/d)$: \mathcal{H}_c is in the range 20–40 when \mathcal{L}/d varies between 10^2 to 10^4 .

Optimal yarn.—The maximum resistance of a yarn is attain for $\mathcal{H} \geq \mathcal{H}_c$, but is it possible to attain this value? Indeed, twisting a yarn elongates the fibers which may break: twisting a yarn too much reduces its strength, a fact already noticed by Galileo [2]. The elongation may be evaluated: a length dz of an initially straight fiber at $r = R$ becomes $ds = dz \sqrt{1 + \gamma^2}$ after the twist of the yarn. The deformation $\varepsilon = (ds - dz) / dz \simeq \gamma^2 / 2$ should be lower than ε_r , so that the twist must verify $\gamma^2 < 2\varepsilon_r$. The maximum attainable value of \mathcal{H} without breaking of fibers is then $\mathcal{H}_r = 2\mu\varepsilon_r \mathcal{L} / R$. For a maximal resistance without breaking due to twist we must have $\mathcal{H}_c \leq \mathcal{H} \leq \mathcal{H}_r$, so that

$$R \leq R_{\text{opt}} = 2\mu\varepsilon_r \mathcal{L} / \mathcal{H}_c, \quad (8)$$

where we introduced R_{opt} as the value of the yarn radius R which verifies $\mathcal{H}_r = \mathcal{H}_c$. R_{opt} is the largest radius of yarn which may reach \mathcal{H}_c without breaking of fibers. For cotton fibers, with $\mathcal{H}_c \simeq 30$, we obtain $R_{\text{opt}} \simeq 80$ μm which is the value of the radius that we measure for our cotton yarn. Thicker simple yarns may be processed, but will not reach their maximal resistance. Making larger yarns with maximal resistance must be done by putting together elementary yarns of radius R_{opt} as it is done in practice [24,25].

Concluding remarks.—From our experiments and our statistical model, a relatively simple picture emerges to properly describe the spinning transition of yarn: the twist on the fiber creates a confining potential. The tangential force variations are then proportional to tension, creating exponential decay of the tension. Although the model is very simple, the experimental variations on model yarns are very well captured. This means that a more refined description of the disorder in the fiber arrays, potential

deviations from helicoidal structures of fibers, or non-linearity arising from non-small curvature ($r \ll p$) are presumably of weak importance.

A crucial result of our study is that the force amplification may be properly described with a single nondimensional number \mathcal{H} that we named Hercules twist number. Although it appears to be a quantity of fundamental interest for the yarn processing, this nondimensional number has apparently not been previously defined. This name echoes to the situation of the interleaved phone book experiment [17,18]. In those studies the authors considered a ‘‘Hercules number’’ $2\mu M^2 \varepsilon / d$, with μ the friction coefficient, M the number of pages, ε the sheet thickness, and d the distance of overlap between leaves. Writing \mathcal{H} as $\mu \theta^2 R / L$, the structure of these two nondimensional numbers appears similar, but with the noticeable difference that θ is controlled by the deformation of the yarn, whereas M is fixed. It should be interesting to investigate in detail if the assembly of frictional objects with different symmetries, such as packing of nonaligned fibers [26] or twisted sheets [27] show similar exponential force variations. Also, it should be interesting to see if recent results on friction effects on bending of layered structures [28] may be extended to fibrous structures.

Finally, it should be noted that our theory is not only qualitative, but also quantitative since $\mathcal{H}_c \simeq 30$ corresponds to the twist value for real yarns. The exponential increases of the force amplification factor $A(\mathcal{H})$, together with the quadratic dependence with the twist angle $\mathcal{H} \sim \theta^2$ induces that the spinning process appears in practice as a sharp twist-controlled phase transition.

*jerome.crassous@univ-rennes1.fr

- [1] B. L. Hardy, M.-H. Moncel, C. Kerfant, M. Lebon, L. Bellot-Gurlet, and N. Mélard, Direct evidence of Neanderthal fibre technology and its cognitive and behavioral implications, *Sci. Rep.* **10**, 4889 (2020).
- [2] G. Galilei, *Discorsi e Dimostrazioni Matematiche, Intorno à due Nuove Scienze Attenenti Alla Meccanica & i Movimenti Locali* (Ludovico Elseviro, Leida, Spain, 1638).
- [3] Birebent, Résistance des fibres végétales filées ou comises, *Ann. Fac. Sci. Toulouse, 3e sér.* **21**, 43 (1929).
- [4] B. Henri, *Cordes et Membranes* (Delagrave, Paris, 1926).
- [5] A. Barella and A. Sust, Cohesion phenomena in cotton rovings and yarns: Part I: General study, *Textile research Journal : publication of Textile Research Institute, Inc and the Textile Foundation* **32**, 217 (1962).
- [6] F. T. Peirce, Tensile tests for cotton yarns, part V: ‘‘The weakest link’’ theorems on the strength of long and of composite specimens, *J. Text. Inst. Trans.* **17**, T355 (1926).
- [7] S. Pradhan, A. Hansen, and B. K. Chakrabarti, Failure processes in elastic fiber bundles, *Rev. Mod. Phys.* **82**, 499 (2010).
- [8] C. Gégauff, Force et élasticité des filés en coton, *Bull. Soc. Ind. Mulhouse* **77**, 153 (1907).
- [9] R. R. Sullivan, A theoretical approach to the problem of yarn strength, *J. Appl. Phys.* **13**, 157 (1942).
- [10] J. W. S. Hearle, Theoretical analysis of the mechanics of twisted staple fiber yarns, *Text. Res. J.* **35**, 1060 (1965).
- [11] R. M. Broughton, Jr., Y. El Mogahzy, Jr., and D. M. Hall, Jr., Mechanism of yarn failure, *Text. Res. J.* **62**, 131 (1992).
- [12] N. Pan, Development of a constitutive theory for short fiber yarns: Mechanics of staple yarn without slippage effect, *Text. Res. J.* **62**, 749 (1992).
- [13] N. Pan, Development of a constitutive theory for short fiber yarns part II: Mechanics of staple yarn with slippage effect, *Text. Res. J.* **63**, 504 (1993).
- [14] P. B. Warren, R. C. Ball, and R. E. Goldstein, Why Clothes Don’t Fall Apart: Tension Transmission in Staple Yarns, *Phys. Rev. Lett.* **120**, 158001 (2018).
- [15] B. Andreotti, Y. Forterre, and O. Pouliquen, *Granular Media: Between Fluid and Solid* (Cambridge University Press, Cambridge, England, 2013).
- [16] Y. Bertho, F. Giorgiutti-Dauphiné, and J.-P. Hulin, Dynamical Janssen Effect on Granular Packing with Moving Walls, *Phys. Rev. Lett.* **90**, 144301 (2003).
- [17] H. Alarcón, T. Salez, C. Poulard, J.-F. Bloch, É. Raphaël, K. Dalnoki-Veress, and F. Restagno, Self-Amplification of Solid Friction in Interleaved Assemblies, *Phys. Rev. Lett.* **116**, 015502 (2016).
- [18] R. Taub, T. Salez, H. Alarcón, É. Raphaël, C. Poulard, and F. Restagno, Nonlinear amplification of adhesion forces in interleaved books, *Eur. Phys. J. E* **44**, 71 (2021).
- [19] J. Crassous (to be published).
- [20] M. van Hecke, Jamming of soft particles: Geometry, mechanics, scaling and isostaticity, *J. Phys. Condens. Matter* **22**, 033101 (2010).
- [21] A. Panaitescu, G. M. Grason, and A. Kudrolli, Measuring geometric frustration in twisted inextensible filament bundles, *Phys. Rev. E* **95**, 052503 (2017).
- [22] W. E. Morton and J. W. S. Hearle, *Woodhead Publishing Series in Textiles*, 4th ed. (Woodhead Publishing Limited, Cambridge, 2008), ISBN 9781845692209.
- [23] R. B. Belser and J. L. Taylor, Frictional properties of cotton fibers, Final report Georgia Tech Project No. A-843, Georgia Institute of Technology (1968), https://smartech.gatech.edu/bitstream/handle/1853/41782/a-843_328310_fr.pdf
- [24] J. W. S. Hearle, P. Grosberg, and S. Backer, *Structural Mechanics of Fibers, Yarns, and Fabrics* (John Wiley & Sons Inc., New York, 1969).
- [25] N. Pan, Exploring the significance of structural hierarchy in material systems—A review, *Appl. Phys. Rev.* **1**, 021302 (2014).
- [26] G. Verhille, S. Moulinet, Nicolas Vandenberghe, M. Adda-Bedia, and P. Le Gal, Structure and mechanics of aegagropilae fiber network, *Proc. Natl. Acad. Sci. U.S.A.* **114**, 4607 (2017).
- [27] J. Chopin and A. Kudrolli, Tensional twist-folding of sheets into multilayered architectures and scrolled yarns, [arXiv:2011.13370](https://arxiv.org/abs/2011.13370).
- [28] S. Poincloux, T. Chen, B. Audoly, and P. M. Reis, Bending Response of a Book with Internal Friction, *Phys. Rev. Lett.* **126**, 218004 (2021).